



## **Gulf Stream Ring Water Intrusion on** the Mid-Atlantic Bight Continental **Shelf Break Affects Microbially Driven Carbon Cycling**

Adrienne Hoarfrost<sup>1\*†</sup>, John Paul Balmonte<sup>1†</sup>, Sherif Ghobrial<sup>1</sup>, Kai Ziervogel<sup>2</sup>,

Department of Marine Sciences, The University of North Carolina at Chapel Hill, Chapel Hill, NC, United States, Institute for the Study of Earth, Oceans, and Space, University of New Hampshire, Durham, NH, United States, 3 Department of Physical Oceanography, Woods Hole Oceanographic Institution, Woods Hole, MA, United States

John Bane<sup>1</sup>, Glen Gawarkiewicz<sup>3</sup> and Carol Arnosti<sup>1</sup>

Développement (IRD), France

Institut de Recherche pour le

**OPEN ACCESS** 

Edited by: Mar Benavides.

Reviewed by:

France Van Wambeke, Centre National de la Recherche Scientifique (CNRS), France X. Antón Álvarez-Salgado, Spanish National Research Council (CSIC), Spain

#### \*Correspondence:

Adrienne Hoarfrost adrienne.hoarfrost@rutgers.edu

#### †Present address:

Adrienne Hoarfrost. Department of Biochemistry and Microbiology, Rutgers University, New Brunswick, NJ, United States John Paul Balmonte, Department of Ecology and Genetics, Uppsala University, Uppsala, Sweden

## Specialty section:

This article was submitted to Aquatic Microbiology, a section of the journal Frontiers in Marine Science

Received: 08 April 2019 Accepted: 25 June 2019 Published: 11 July 2019

#### Citation:

Hoarfrost A, Balmonte JP, Ghobrial S, Ziervogel K, Bane J, Gawarkiewicz G and Arnosti C (2019) Gulf Stream Ring Water Intrusion on the Mid-Atlantic Bight Continental Shelf Break Affects Microbially Driven Carbon Cycling. Front. Mar. Sci. 6:394. doi: 10.3389/fmars.2019.00394

Warm core, anticyclonic rings that spin off from the Gulf Stream circulate through the region directly offshore of the Mid-Atlantic Bight. If a warm core ring reaches the continental shelf break, its warm, highly saline water may subduct under cooler, fresher continental shelf surface water, resulting in subsurface waters at the shelf break and over the upper continental slope with high temperatures and salinities and distinct physical and chemical properties characteristic of Gulf Stream water. Such intruding water may also have microbial communities with distinct functional capacities, which may in turn affect the rate and nature of carbon cycling in this coastal/shelf environment. However, the functional capabilities of microbial communities within ring intrusion waters relative to surrounding continental shelf waters are largely unexplored. We investigated microbial community capacity to initiate organic matter remineralization by measuring hydrolysis of a suite of polysaccharide, peptide, and glucose substrates along a transect oriented across the Mid-Atlantic Bight shelf, shelf break, and upper slope. At the outermost sampling site, warm and salty water derived from a Gulf Stream warm core ring was present in the lower portion of the water column. This water exhibited hydrolytic capacities distinct from other sampling sites, and exhibited lower heterotrophic bacterial productivity overall. Warm core rings adjacent to the Mid-Atlantic Bight shelf have increased in frequency and duration in recent years. As the influence of warm core rings on the continental shelf and slope increases in the future, the rate and nature of organic matter remineralization on the continental shelf may also shift.

Keywords: warm core ring, ring intrusion, Mid-Atlantic Bight, heterotrophy, carbon cycling, enzymatic activity

## INTRODUCTION

Western boundary currents often influence adjacent or nearby continental shelf areas. The Mid-Atlantic Bight (MAB) continental shelf off the northeastern United States stretches from Cape Hatteras to Georges Bank, and this region is repeatedly affected by warm core rings that have spun off from the Gulf Stream (e.g., Joyce et al., 1992; Gawarkiewicz et al., 2001; Chen et al., 2014; Zhang and Gawarkiewicz, 2015). Warm core rings are a type of oceanic mesoscale eddy, and

1

numerous such rings are formed on the north side of the Gulf Stream each year. They are composed of Gulf Stream water that is circulating anti-cyclonically, and they typically drift to the north and west, where many eventually encounter the upper continental slope and outer continental shelf along the MAB.

In recent years, there have been instances in which the path of the Gulf Stream jet has shifted well north of its normal meander envelope and thus is in close proximity to the shelf break and outer continental shelf (Gawarkiewicz et al., 2012; Ezer et al., 2013; Ullman et al., 2014). Such shifts in ocean water circulation have the potential to profoundly affect the biological framework of life in the ocean. For example, upwelling of nutrient-rich deep water to the euphotic zone at the shelfbreak front in the MAB leads to enhanced primary productivity within the shelfbreak front and jet (Chen and He, 2010; Zhang et al., 2013). Such interactions between physical and biological processes have long been understood as the foundation of the ocean's food web (Redfield, 1958; McGillicuddy, 2015). Understanding of finer-scale ocean circulation interactions with the shelf is less mature, in part because development of the instruments and capabilities to make higher resolution observations of relevant ocean parameters over sufficiently large temporal and spatial scales has occurred comparatively recently. In the last several years, however, new observational capabilities such as the Ocean Observatories Initiative's Pioneer Array have highlighted increased exchange across the shelf break and the importance of warm core rings over the upper continental slope (Gawarkiewicz et al., 2018).

Recent studies have suggested that Gulf Stream influences on the continental shelf and slope south of New England have been increasing. Andres (2016) found that the initiation region for large amplitude Gulf Stream meanders has been shifting steadily westward since 1995 and large amplitude meanders are now occurring west of the New England Seamount Chain. Furthermore, the number of warm core rings formed annually has increased by roughly 50% for the time frame 2000-2016 compared to 1977-1999 (Monim, 2017). Repeated cross-shelf glider transects from the Pioneer Array have shown that the mean salinity over the continental slope during a 2 years time period was 35.7 PSU, an increase of over 0.6 PSU relative to slope water mass properties from the 1970s and earlier (Gawarkiewicz et al., 2018). Additionally, while previous investigations of the presence of ring intrusions on the continental shelf showed strong seasonal dependence (Lentz, 2003), with a peak in August and negligible frequency of intrusions in April, in recent years ring intrusions have been shown to occur throughout the year. For example, Gawarkiewicz et al. (2018) document a ring intrusion extending onshore from the shelfbreak to the 30 m isobath in January 2017. A recent census of warm core rings in the Northwest Atlantic indicates a peak in formation between 65° and 70° West in July of ca. 0.75 rings/year, and ca. 0.6 rings/year in April, with ca. 3 rings/year in the region from 55 to 75° West, and ca. 2 rings/year in April (Etige, 2019).

Warm, salty waters intruding onto the upper slope and outer shelf can bring ecosystem changes. For example, new species have been documented on the continental shelf during seasons in which they are not normally present (Gawarkiewicz et al., 2018).

However, the effects of such intrusions on biogeochemical cycling are just beginning to be investigated. The activities of heterotrophic microbial communities are particularly important in this respect, since they are key drivers of carbon and nutrient cycling, transforming and remineralizing organic matter, and generating new biomass. These processes function as a constraint on the amount of carbon recycled to the atmosphere as CO<sub>2</sub> or transported to deeper water depths (Azam and Malfatti, 2007; Falkowski et al., 2008). The functional capabilities of microbial communities in warm core ring features, and the timing and persistence of such rings along the continental shelf and slope, thus may affect the location and rate of carbon cycling along this portion of the ocean margin.

The carbon-cycling activities of microbial communities are initiated by extracellular enzymes, which hydrolyze high molecular weight (HMW) organic matter into sizes sufficiently small to be transported into the cell. The assemblage of enzymes that a microbial community can produce affects the nature and quantity of organic substrates that microbial communities can access, as well as the rates at which they are hydrolyzed (Arnosti, 2011). These functional patterns follow gradients across depth (Baltar et al., 2010b; Steen et al., 2012; Hoarfrost and Arnosti, 2017), latitude (Arnosti et al., 2011), hydrographic properties (Baltar and Arístegui, 2017; Hoarfrost and Arnosti, 2017; Balmonte et al., 2018), and between coastal and open ocean regions (D'Ambrosio et al., 2014).

Distinct hydrolytic capacities of microbial communities within water masses result in different rates of carbon degradation in different regions of the ocean, often most obviously where boundaries between water masses are sharp (Baltar and Arístegui, 2017). Gulf Stream warm core rings may transport a distinct microbial community with distinct hydrolytic capacities (Baltar et al., 2010a). These distinct functional capacities may affect carbon cycling over the MAB outer shelf and upper slope during intrusions of ring-derived waters there; however, this possibility has not yet been investigated.

Recent years have brought increased use of new sensors, gliders, and floats that provide continuous physical and chemical data, enabling high-resolution spatial and temporal tracking of specific water masses, including observation of the increased frequency of ring intrusions on the shelf (Andres, 2016; Gawarkiewicz et al., 2018). In contrast, continuous and/or highresolution measurements of microbial extracellular enzymatic activities - the initial step of carbon cycling -with similar spatial and temporal resolution is not yet possible. Although high-resolution automated collection of samples of microbial transcripts provides new insight into microbial dynamics (e.g., Ottesen et al., 2014; Aylward et al., 2015), rates of processes cannot be inferred from such samples. Here we focus instead on ship-based sampling and incubation of "end points" of ring intrusion, by comparing microbial community activities in surface and bottom waters on a transect along the MAB shelf and shelf break during a ring intrusion event. This transect included stations spanning shelf water, slope water, and ring-derived water. Measurement of microbial activities - potential activities of enzymes hydrolyzing peptides and polysaccharides, as well as heterotrophic bacterial productivity - across these distinct

137 ± 24 120 ± 27 81 ± 9 90 ± 6 78 ± 7 89 ± 9 64 ± 5

water masses yields insight into the biogeochemical capabilities of microbial communities associated with interactions between the Gulf Stream and the continental shelf of the Mid-Atlantic Bight.

## **MATERIALS AND METHODS**

Hydrographic sampling was conducted with a SeaBird 911+CTD fromthe R/V Endeavor between April 27 and 28, 2015 (cruise EN556). Vertical profiles were sampled at four stations between the 63 m and 207 m isobaths roughly along 71°W. Station 1 was located at 40.71°N 71.03°W, Station 2 at 40.46°N 71.00°W, Station 3 at 40.31°N 71.00°W, and Station 4 at 40.07°N 71.01°W (Table 1 and Supplementary Figures 1, 2). Water masses were identified (see section "Results") based on temperature and salinity characteristics, as well as the observation of warm core ring movements from satellite sea surface temperature observations in this region before, during, and after the time period of sampling.

## **Seawater Collection**

Seawater was collected from 1 m below surface and within a few meters of the bottom at each station using a Niskin rosette equipped with a CTD sensor. Bottom sampling depths were 58 m (Stn. 1), 78 m (Stn. 2), 97 m (Stn. 3), and 199 m (Stn. 4; Table 1). Seawater was transferred to 20 L carboys that were rinsed three times with water from the sampling depth and then filled with seawater from a single 30 L Niskin bottle, using silicone tubing that had been acid washed then thoroughly rinsed with distilled water prior to use. From each carboy, water was dispensed into smaller 1-2 L glass containers that were cleaned and pre-rinsed three times with water from the carboy prior to dispensing. This water was used to measure heterotrophic bacterial productivity and the activities of polysaccharide hydrolases, peptidases, and glucosidases. One separate glass 1 L Duran bottle was filled with seawater from the carboy and sterilized in an autoclave for 20-30 min to serve as a killed control for microbial activity measurements. Note that the experiments carried out with this water - in particular, measurement of polysaccharide hydrolase activities - are resource- and time-consuming to set up and carry out subsequent analyses. For this reason, collection and incubation of additional depths and locations was not possible during the short duration of this transect: the eight depths/locations reported here represent the maximal possible effort by the shipboard party.

## Incubation Setup and Subsampling – Peptidases and Glucosidases

The hydrolysis of seven low molecular weight substrate proxies was measured in surface and bottom waters from all four stations. Two substrates,  $\alpha$ -glucose and  $\beta$ -glucose linked to a 4-methylumbelliferyl (MUF) fluorophore, were used to measure glucosidase activities. Five substrates linked to a 7-amido-4-methyl coumarin (MCA) fluorophore, one amino acid – leucine – and four peptides – the chymotrypsin substrates alanine-alanine-phenylalanine (AAF) and alanine-alanine-proline-phenylalanine (AAPF), and the trypsin substrates glutamine-alanine-arginine

	Latitude (°N)	Longitude (°E)	Bottom depth (m)	Sampling depth (m)	Sampling date (DD/MM/YYYY)	Incubation temp (°C)	In situ temp (°C)	In situ salinity (PSU)	In situ oxygen (ml L <sup>-1</sup> )	In situ Chla (mg m³ -1)	Leu incorp. (pM/h)	Bact prod. (ng C L <sup>-1</sup> h <sup>-1</sup> )	
Stn. 1 surface	40.7071	-71.028	63	-	27/04/2015	80	5.7	32.8	7.2	0.38	13 ± 2	23 ± 3	-
Stn. 1 bottom	40.7071	-71.028	63	58	27/04/2015	4	3.6	33.1	6.7	0.84	20 ± 5	36 ± 9	_
Stn. 2 surface	40.4622	-71.0008	83.6	-	27/04/2015	80	6.3	33.1	7.1	0.67	21 ± 5	38 ± 9	_
Stn. 2 bottom	40.4622	-71.0008	83.6	78	27/04/2015	4	4.7	33.4	6.5	0.68	21 ± 5	38 ± 9	
Stn. 3 surface	40.3084	-71.0048	102	-	28/04/2015	80	7.8	33.4	7.2	1.09	42 ± 4	76 ± 7	
Stn. 3 bottom	40.3084	-71.0048	102	26	28/04/2015	8	10.5	35.1	4.7	0.42	7 ± 3	13 ± 6	
Stn. 4 surface	40.0702	-71.0052	206.9	-	28/04/2015	80	7.7	33.4	7.3	0.78	92 ± 8	166 ± 14	
Stn. 4 bottom	40.0702	-71.0052	206.9	199	28/04/2015	14	12.0	35.6	4.7	0.34	3 # 1	5 ± 1	

(QAR) and phenylalanine-serine-arginine (FSR) – were used to measure exo- and endo-acting peptidase activities, respectively. These substrates collectively are derived from two major classes of organic matter, carbohydrates ( $\alpha$ -glucose and  $\beta$ -glucose) and amino acids that are constituents of proteins (leucine, QAR, FSR, AAF, and AAPF). Furthermore, these substrates are cleaved by enzymes that hydrolyze their substrates in two distinct patterns: exo-acting enzymes (cleaving end-terminus residues:  $\alpha$ -glucose,  $\beta$ -glucose, and leucine) and endo-acting enzymes (mid-chain cleaving: QAR, FSR, AAF, and AAPF). As with the polysaccharide substrate incubations, these substrates were incubated at saturating concentrations and thus measure potential enzymatic activities.

Hydrolysis rates of the substrates were measured as an increase in fluorescence as the fluorophore was hydrolyzed from the substrate over time (after Hoppe, 1983; Obayashi and Suzuki, 2005). Incubations with the seven low molecular weight substrates were set up in a 96-well plate. For each substrate, triplicate wells were filled with a total volume of 200 µL seawater for experimental incubations; triplicate wells were filled with 200 µL autoclaved seawater for killed control incubations. Substrate was added at saturating concentrations. A saturation curve was determined with surface water from each station to determine saturating concentrations of substrate. Saturation curve incubations were conducted with leucine and β-glucose substrates, and as saturating concentrations were found to be similar for both substrates, this concentration was used as the saturating concentration for all glucosidase and peptidase substrates. The saturating concentration was identified as the lowest tested concentration of substrate at which additional substrate did not yield higher rates of hydrolysis. Fluorescence was measured over 24 h incubation time with a plate reader (TECAN spectrafluor plus; 360 nm excitation, 460 emission), with timepoints taken every 4-6 h. Hydrolysis rates were calculated from the rate of increase of fluorescence in the incubation over time relative to a set of standards of known concentration of fluorophore. The similarity of the spectra of glucosidase and peptidase substrates hydrolyzed among sampling sites were calculated as with polysaccharide substrates, using the Jaccard similarity metric and testing statistical significance with PERMANOVA.

Scripts to calculate hydrolysis rates and produce the figures shown here are available in the associated Github repository (Hoarfrost, 2017).

# Incubation Setup and Subsampling – Polysaccharide Hydrolases

The potential of the pelagic microbial community to hydrolyze six HMW polysaccharides (arabinogalactan, chondroitin sulfate, fucoidan, laminarin, pullulan, and xylan) was investigated in surface and bottom water at all four stations using fluorescently labeled polysaccharides (Arnosti, 1996, 2003). These substrates were chosen for their diverse molecular structure, and because they are all found in the marine environment and/or enzymes able to target these polysaccharides are present in marine

microorganisms (e.g., Alderkamp et al., 2007; Martinez-Garcia et al., 2012; Wegner et al., 2013).

For each substrate, three 50 mL falcon tubes were filled with seawater and one 50 mL falcon tube was filled with autoclaved seawater to serve as a killed control. Substrate was added at 3.5 µM monomer-equivalent concentrations, except for fucoidan, which was added at 5 μM concentrations (a higher concentration was necessary for sufficient fluorescence detection). These substrate concentrations represent a ca. 20 µM C increase in dissolved organic carbon (DOC) naturally present in seawater. Since the added substrates are in competition with any naturally occurring polysaccharides for enzyme active sites, our measured hydrolysis rates are potential activities. Two 50 mL falcon tubes - one with seawater and one with autoclaved seawater - with no added substrate served as blank controls. Incubations were stored in the dark at as close to in situ temperature as possible, given the finite number of temperaturecontrolled incubators aboard ship (Table 1).

Subsamples of the incubations were collected at time zero, and at six subsequent timepoints (t1–t6): 2, 5, 10, 17, 30, and 42 days. These timepoints were chosen based on previous experience, since it is impossible to know *a priori* at what timepoint hydrolytic activity can be detected. Here, we report the data from the first three timepoints (2, 5, and 10 days), since all activities that were detectable throughout the timecourse of incubation were detected by the 10 days timepoint. At each timepoint, 2 mL of seawater was collected from the 50 mL falcon tube using a sterile syringe, filtered through a 0.2  $\mu$ m pore size syringe filter, and stored frozen until processing; the 50 mL falcon tube was replaced at its previous temperature to continue incubation.

The hydrolysis of HMW substrate to lower molecular weight hydrolysis products was measured using gel permeation chromatography with fluorescence detection, after the method of Arnosti (1996, 2003). In short, the subsample was injected onto a series of columns consisting of a 21 cm column of G50 and a 19 cm column of G75 Sephadex gel. The fluorescence of the column effluent was measured at excitation and emission wavelengths of 490 and 530 nm, respectively. Hydrolysis rates were calculated from the change in molecular weight distribution of the substrate over time, as described in detail in Arnosti (2003). The pairwise similarity of the spectra of polysaccharide substrates hydrolyzed among sampling sites was calculated using the Jaccard similarity metric, and the statistical significance of the differences in hydrolytic spectra among the shelf, slope, and ring-intrusion water masses was evaluated with a PERMANOVA test.

Scripts calculating hydrolysis rates and producing the figures depicted in this manuscript are available at the associated Github repository (Hoarfrost, 2017).

## Heterotrophic Bacterial Productivity Measurements

Heterotrophic bacterial protein production was measured via <sup>3</sup>H-leucine incorporation by heterotrophic bacteria using the cold trichloroacetic acid (TCA) and microcentrifuge extraction method (after Kirchman, 2001). All work was performed aboard ship. In brief, triplicate live samples of 1.5 mL seawater as

well as one 5% (w/v) TCA-killed control were incubated with 23 µL of 1 mCi/mL L-[3,4,5-3H(N)]-Leucine (PerkinElmer, 100-150 Ci/mmol specific activity, NET460250UC) to a final concentration of 20 nM for between 4 and 24 h in the dark at as close to in situ temperature as possible. Live samples were then killed with 89 µL of 100% (w/v) TCA and centrifuged (10,000 rpm at 4°C for 10 min) to pelletize cell material. The supernatant liquid was removed and 1 mL of 5% (w/v) TCA solution was added, followed by vortex mixing and centrifugation. Supernatant removal, mixing, and centrifugation were repeated using 1 mL of 80% ethanol solution. Finally, the supernatant liquid was removed and each sample was dried overnight. After drying, 1 mL of scintillation cocktail (ScintiSafe 30% Cocktail, Fisher SX23-5) was added and incorporated radioactivity was measured using a LSA scintillation counter (PerkinElmer Tri-Carb 2910TR). Leucine incorporation rate was calculated from the incorporated radioactivity, compared to 1 mL of scintillation cocktail spiked with 23 µL of L- $[3,4,5-{}^{3}H(N)]$ -Leucine radioactivity, divided by incubation time. Rates of heterotrophic bacterial productivity were calculated with a conversion factor of 1.8 kg C mol Leu-1 after (Azam and Simon, 1989).

## Dissolved Organic Carbon Measurements

Water samples for DOC measurements were collected from the Niskin bottles immediately after retrieval, before any other sampling took place. Clean and acid washed syringes, tubing, and filter holders were used for each sampling. Duplicate DOC samples were filtered using the same 60 mL syringe through combusted glass fiber filters (Whatman 1825-025) secured within a polycarbonate filter holder into two combusted 20 mL scintillation vials, acidified using 100  $\mu$ L of 50% phosphoric acid, then immediately frozen at  $-20^{\circ}$ C. DOC samples were analyzed by high temperature catalytic oxidation (HTCO) using a Shimadzu Total Organic Carbon analyzer (TOC-8000A/5050A).

## **RESULTS**

## **Water Masses Sampled**

Overviews of T-S characteristics that define water masses in this region appear in Wright and Parker (1976), Linder and Gawarkiewicz (1998) and Lentz (2003). Key water masses include shelf water (T typically  $10^{\circ}$ C or below and S less than  $\sim 34.5$  PSU), slope water (T  $\sim 10$  to  $12^{\circ}$ C, S  $\sim 34.5$  to 35.5) and warm core ring water (S  $\sim 35.5$  PSU or greater). Salinities within warm core rings can be 36.0 PSU or higher shortly after formation. The temperature-salinity (T-S) properties from Stns. 1-4 reveal the water masses that were present along the section at the time of sampling.

Temperature and salinity characteristics as well as water masses characterizing the transect are shown in **Figure 1**. Stns. 1 and 2 were occupied solely with shelf water. The upper water column at Stns. 3 and 4 also had temperature and salinities typical of shelf water, although both T and S were slightly higher than at Stns. 1 and 2. The salinity near the bottom in

Stn. 3 was above 35 PSU, which is typical of slope water that includes mixtures of shelf water and warm core ring water. The salinity for Stn. 4 was over 35.5 PSU from 120 m depth to the bottom of the profile, indicating properties of a warm core ring water mass (**Table 1** and **Figure 1**). DOC was highest at Stns. 1 and 2 surface (120–135  $\mu$ M), with decreasing concentrations offshore (80–90  $\mu$ M at Stn. 2 bottom, Stn. 3, and Stn. 4 surface), and the lowest measured DOC concentrations at Stn. 4 bottom (63.5  $\mu$ M) (**Table 1**).

Satellite sea surface temperature (SST) images from the dates leading up to and during sampling of the four stations show two warm core Gulf Stream rings in the region, one to the southwest (RING) and one to the southeast (RING-2) of Stn. 4 (Figure 1D and Supplementary Figure 1). RING-2 was propagating westward, approaching the survey line during April 22-29. On April 27-28, the dates of sampling, the activity of this ring appears to have "pushed" a warm water filament toward the survey line. The surface expression of the filament is apparent in the SST image of April 28 (Figure 1). The existence of water below 120 m at Stn. 4 with ring T-S characteristics is likely the deep expression of this filament. Since the deeper water was ahead (i.e., to the west) of the leading edge of the filament location on April 28, this would have required the deeper water to be flowing westward somewhat faster than the surface filament water. This would be a deep velocity vector pointing out of the page in Figure 1C, which we suggest with a "circle-dot" vector in the T and S sections. Such westward flow in the deep waters of Stn. 4 (Figure 1C) is consistent with a thermal-wind shear due to the sloping density surfaces within the slope and ring waters, shown in these sections.

## **Heterotrophic Bacterial Productivity**

Heterotrophic bacterial productivity was particularly low in Stns. 3 and 4 bottom water, at 13 and 5 ng C  $\rm L^{-1}~h^{-1}$ , respectively, but was considerably higher in surface water of the same stations, at 76 and 166 ng C  $\rm L^{-1}~h^{-1}$ , respectively (**Table 1**). At Stns. 1 and 2, there was less difference between surface and bottom waters, and heterotrophic bacterial productivity was moderate compared to Stns. 3 and 4, ranging from 23 to 38 ng C  $\rm L^{-1}~h^{-1}$ .

## Peptidase and Glucosidase Activities

Differences in the spectrum of peptide and glucose substrates hydrolyzed, as well as hydrolysis rates, were notable among shelf and shelf break water masses (Figure 2; note difference in y axes for Stns. 1 and 2 compared to Stns. 3 and 4). At Stns. 1 and 2, which corresponded with Cold Pool shelf waters, comparatively few substrates were hydrolyzed, and activities were quite low, ranging between 0 and 5.2 nmol  $L^{-1}$   $h^{-1}$ . At these two stations, activities were dominated by hydrolysis of QAR-trypsin and either AAF-chymotrypsin (Stn. 2; Stn. 1 bottom water) or α-glucose (Stn. 1 surface water). Nearer the shelf break, Stns. 3 and 4 showed a much wider spectrum of activities and considerably higher hydrolysis rates. The surface warm shelf waters of Stns. 3 and 4, which had similar physical characteristics to each other (Figure 1A), also showed similar hydrolysis profiles, dominated by leucine amino peptidase activities averaging 79-88 nmol L-1 h-1,

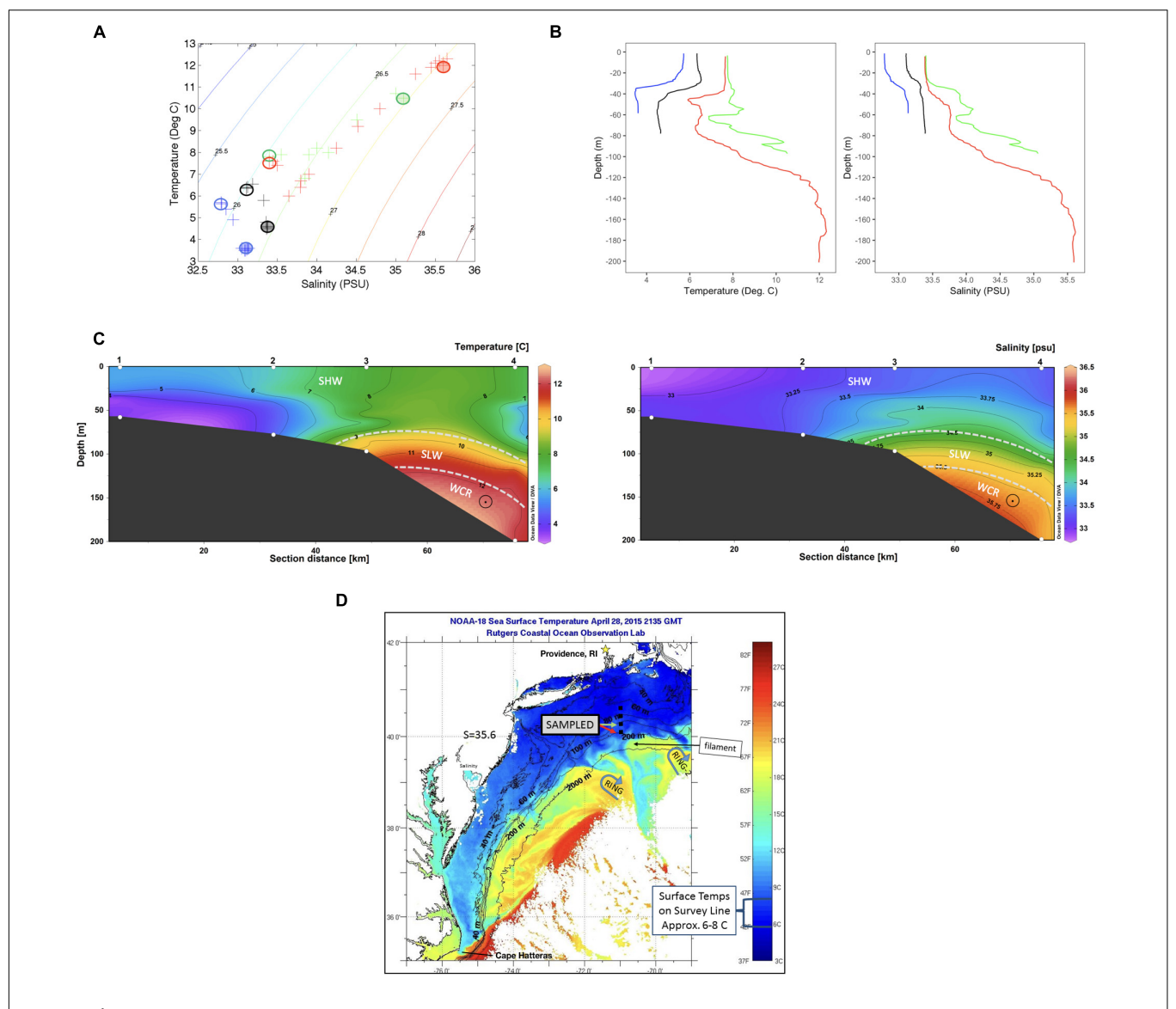


FIGURE 1 (A) A temperature/salinity plot identifying water mass characteristics from the four stations. Sampling locations indicated by circles, filled circles bottom and empty circles surface waters. (B) Temperature (left) and salinity (right) profiles at each station (data from CTD). Blue: Stn. 1; Black: Stn. 2; Green: Stn. 3; Red: Stn. 4. (C) Vertical contour of temperature and salinity over the sampling transect, with water masses sampled indicated by dashed lines. SHW, Shelf water; SLW, Slope water; WCR, Warm core ring intrusion. (Plot produced with Ocean Data View, Schlitzer, 2016). (D) Satellite imagery of sea surface temperature on April 28, the day Stns 3 and 4 were sampled. Stations surveyed are indicated by black squares. Two warm core rings near the survey sites are indicated by blue arrows, and a warm filament being pushed onto the continental shelf where Stn. 4 bottom waters are sampled is indicated.

with trypsin (QAR, FSR) and chymotrypsin (AAF, AAPF) activities ranging between 4 and 21 nmol  $L^{-1}\ h^{-1}$ , and very low but detectable levels of  $\alpha$ - and  $\beta$ -glucosidase activity. Bottom waters of Stn. 3, corresponding to slope waters, showed lower leucine aminopeptidase activity (24.1 nmol  $L^{-1}\ h^{-1}$ ) compared to surface water from the same station; activities of QAR-trypsin (at 24.1 nmol  $L^{-1}\ h^{-1}$ ) were, however, higher than in surface water of Stn. 3. At Stn. 3 (both depths) as well as surface water of Stn. 4, all of the peptidase and glucosidase substrates were hydrolyzed. In Stn. 4 bottom water, corresponding to the warm core ring derived filament, however, a much narrower spectrum of activities was measured: no FSR,

AAF, or  $\alpha$ -glucose were hydrolyzed. This narrow spectrum of activities did not translate to low hydrolysis rates for the other substrates, however, since leucine aminopeptidase activity was 21.7 nmol L<sup>-1</sup> h<sup>-1</sup>, and AAPF-chymotrypsin and QAR-trypsin activities were 12.7 and 4.4 nmol L<sup>-1</sup> h<sup>-1</sup>, respectively (**Figure 2**). Statistical analysis demonstrated that the spectrum of peptide and glucose substrates hydrolyzed differed according to water mass source, with significantly different Jaccard similarities of hydrolytic spectra between Stns. 1 and 2 Cold Pool shelf waters, Stn. 3 and 4 surface warm shelf waters, Stn. 3 bottom slope waters, and Stn. 4 bottom warm core ring-derived waters (PERMANOVA P = 0.006).

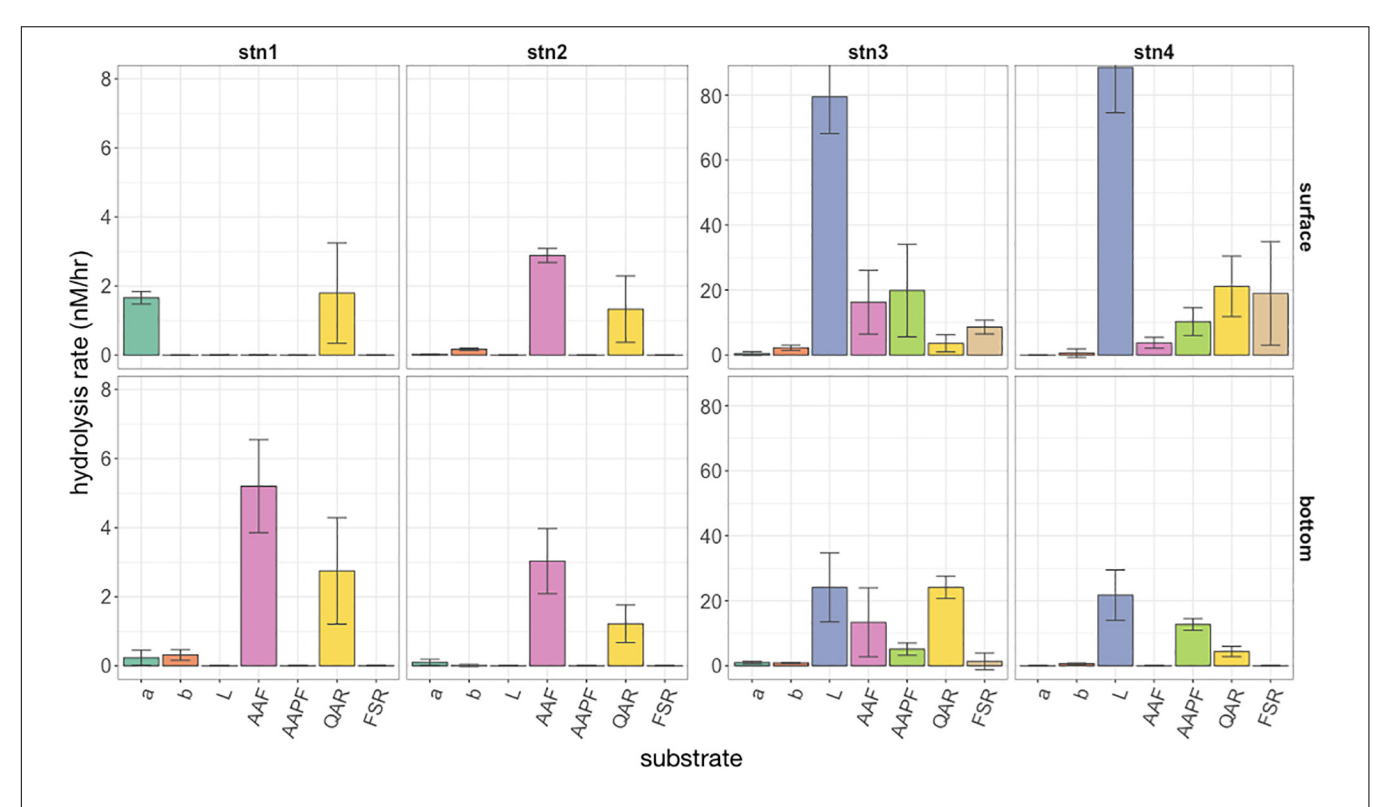


FIGURE 2 | Hydrolysis rate of the seven fluorescently labeled peptide and glucose substrates at each station (left to right) and surface and bottom (top and bottom panels). A-glu, α-glucose; B-glu, β-glucose; Leu, leucine; AAF, alanine-alanine-phenylalanine; AAPF, alanine-alanine-proline-phenylalanine; QAR, glutamine-alanine-arginine; FSR, phenylalanine-serine-arginine. Note the order of magnitude difference in y axes between Stns. 1 and 2 and Stns. 3 and 4. Error bars indicate standard deviation of triplicate incubations around the mean hydrolysis rate.

## **Polysaccharide Hydrolase Activities**

Polysaccharide hydrolase activities, measured initially after 48 h incubation, also showed distinct differences among stations and depths in the spectrum of substrates hydrolyzed, as well as in hydrolysis rates (Figure 3). These hydrolytic spectra were significantly different among cold pool shelf (Stns. 1 and 2), warm shelf break (Stns. 3 and 4 surface), slope (Stn. 3 bottom), and ring derived (Stn. 4 bottom) water masses (PERMANOVA P = 0.048). Activities were considerably higher at Stn. 2 than at the other three stations (summed activities of 26.7 and 44.7 nmol monomer  $L^{-1}$   $h^{-1}$  for surface and bottom water, respectively), and were dominated by chondroitin hydrolysis. As with peptidase and glucosidase activities, Stns. 3 and 4 surface waters also had similar polysaccharide hydrolysis profiles: chondroitin, laminarin, pullulan, and xylan were hydrolyzed at both sites in similar proportions. Summed hydrolysis rates were lowest in bottom waters at Stns. 3 and 4 (1.7 and 5.0 nmol monomer  $L^{-1}$  h<sup>-1</sup>, respectively), although their hydrolysis profiles differed: arabinogalactan, chondroitin, and laminarin were hydrolyzed in Stn. 3 bottom water, while fucoidan, laminarin, pullulan, and xylan were hydrolyzed in Stn. 4 bottom water. Fucoidan and arabinogalactan were only hydrolyzed in bottom waters, while pullulan was only hydrolyzed in surface waters and the bottom waters at Stn. 4.

Given the duration of the polysaccharide incubations, the timecourse of substrate hydrolysis provides additional

information about the response of a microbial community to specific polysaccharides, since multi-day incubations allow sufficient time for enzyme induction, as well as growth responses. Rapid hydrolysis suggests that a large fraction of a microbial community can hydrolyze a substrate or that the active portion of the community is able to respond quickly and at high capacities, while hydrolysis that develops late in a timecourse indicates an activity carried out by a small or slow-growing fraction of the community. Substrate hydrolysis patterns and response times to the six polysaccharides evolved considerably over a 10 days incubation period across substrate, depth, and location (Figure 4) such that the composition of activities at day 10 across sites was significantly different than the composition of activities at day 2 (ANOSIM P < 0.01). Over this time frame, hydrolysis of chondroitin and laminarin became evident in all incubations and generally became an increasing proportion of total polysaccharide hydrolysis over time. Pullulan was rapidly hydrolyzed in all surface waters, but only in bottom waters at Stn. 4. Arabinogalactan was only hydrolyzed in bottom waters, and only at Stns. 1 and 3.

## **DISCUSSION**

The frequency of warm core rings in the slope region south of New England has increased in recent years. In November

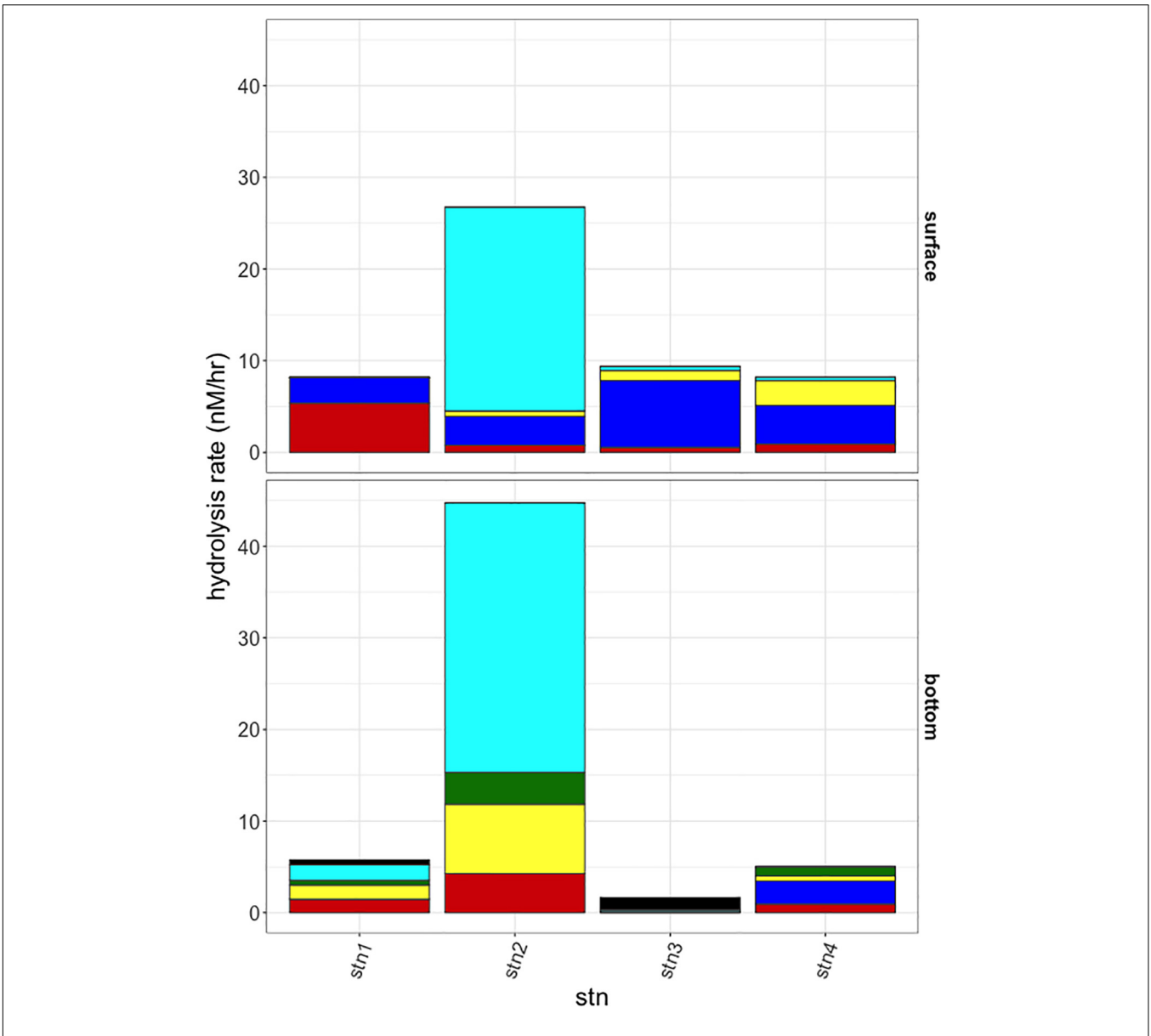
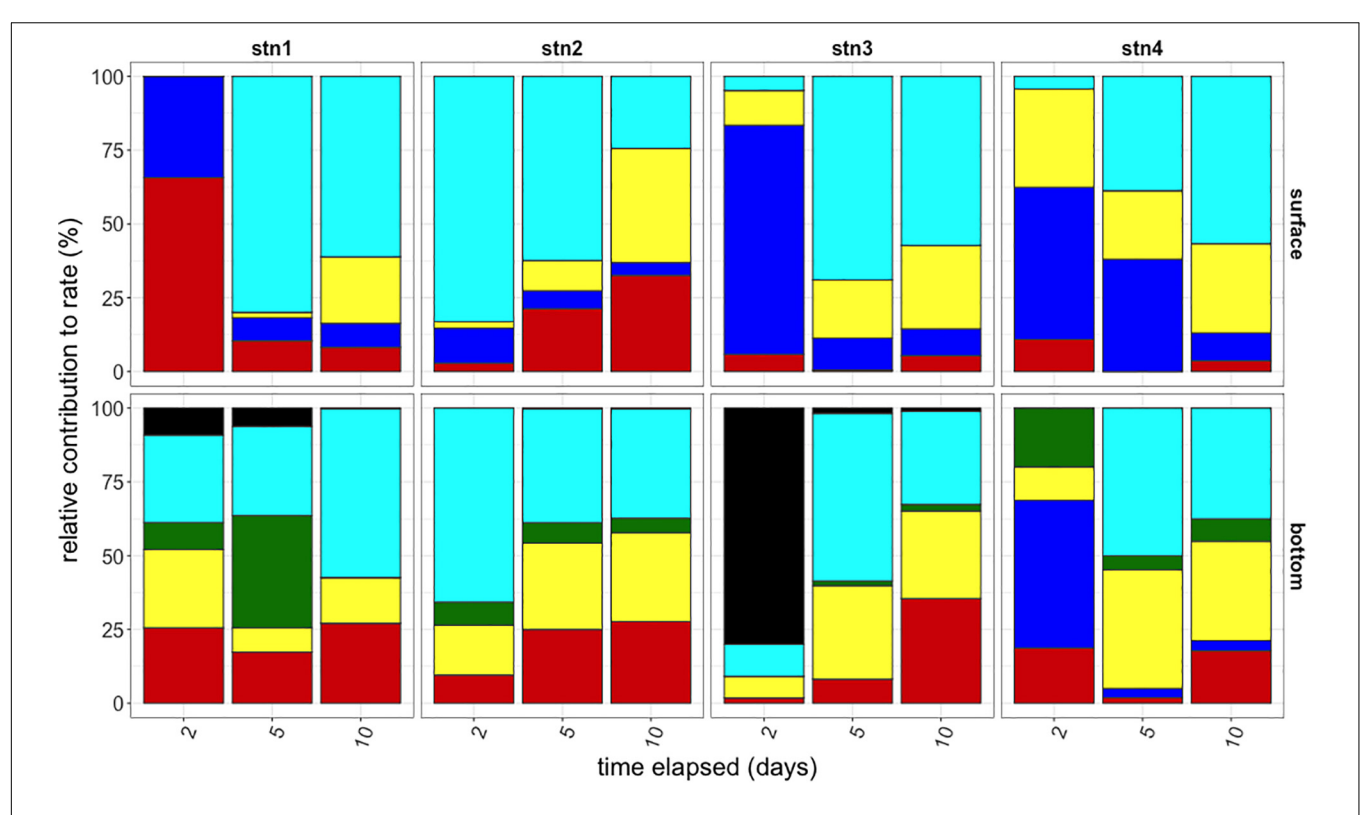


FIGURE 3 | Hydrolysis rates at the 48 h sampling timepoint for the six polysaccharide substrates at each station (left to right) and surface and bottom (top and bottom panels). Black: arabinogalactan; Turquoise: chondroitin sulfate; Green: fucoidan; Yellow: laminarin; Blue: pullulan; Red: xylan.

2009 (Ullman et al., 2014) and December 2011 (Gawarkiewicz et al., 2012), the North Wall of the Gulf Stream was in close proximity to the shelf break south of New England. Observations from the National Marine Fisheries Service, as part of the ECOsystems MONitoring program, have shown that ring water extended shoreward across most of the continental shelf in September 2014 (Gawarkiewicz et al., 2018). More recently, the Ocean Observatories Initiative Pioneer Array identified a large cross-shelf intrusion of ring water in January 2017. Our study identifies a ring intrusion event on the continental slope during the time of sampling in April 2015. We detect distinct biogeochemical characteristics among water masses along the northern part of the MAB during this ring intrusion, and

explore the effect of these events on microbially driven carbon cycling in this region.

A pattern in microbial carbon cycling capacity unique to warm core ring intrusions has implications for carbon biogeochemistry within warm core rings, and in particular on the biogeochemical cycling capacities of the continental shelf during ring intrusions. Across distinct water masses sampled from the continental shelf, shelf break, slope, and the Gulf Stream derived ring (Figure 1), microbial communities demonstrated differences in the spectrum and rates of hydrolysis of a suite of high- and low-molecular-weight organic substrates, as well as in heterotrophic bacterial productivity, indicative of differences in carbon cycling capacities. Gulf Stream derived ring water in the lower reaches



**FIGURE 4** | Relative contributions of polysaccharide hydrolase activities to summed hydrolysis rates (*y*-axis) at the time of subsampling (*x*-axis) for each station (left to right) and depth (top and bottom). Black: arabinogalactan; Turquoise: chondroitin sulfate; Green: fucoidan; Yellow: laminarin; Blue: pullulan; Red: xylan.

of Stn. 4 in particular was distinct from other water masses sampled at other stations and depths, and it was characterized by particularly low heterotrophic bacterial productivity (**Table 1**), the capacity to hydrolyze fewer peptide substrates relative to surface waters at the same station (**Figure 2**), and distinct polysaccharide hydrolase activities (**Figure 3**) as well as peptide and glucose substrate spectra (**Figure 2**). The hydrolytic pattern in the deep, ring water at Stn. 4 contrasted with the other sites sampled on the shelf and slope, whose hydrolytic spectra and hydrolysis rates significantly different from Stn. 4 bottom ring water. Shelf and slope waters were also characterized by widely different rates of heterotrophic bacterial productivity, with particularly high productivity in shelf water at Stn. 3 (**Figure 1A** and **Table 1**).

Differences in functional capacities were evident over long as well as short time-scales, as determined by incubations that reflect the capacity of the microbial community to respond to addition of specific polysaccharides. Even after 10 days of incubation, during which a significant growth response is possible, some polysaccharides were not hydrolyzed (**Figure 4**), indicating that the microbial community as a whole lacked the ability to hydrolyze particular substrates, either because they lacked the genes that encode the necessary enzymes or because such genes were not activated during the incubation. Hydrolytic capacities in water from the warm core ring intrusion, and the timecourse over which different substrates were hydrolyzed most rapidly, were distinct from other sampling sites of shelf and shelf break

waters (**Figure 4**). This observation suggests that the timing and persistence of ring intrusions may also influence the spectrum of organic matter hydrolyzed by microbial communities *in situ*.

We note, moreover, that the hydrolytic patterns differentiating shelf, slope, and ring intrusion water masses are not driven by simple temperature relationships. The significantly higher temperature of the ring intrusion at Stn. 4 bottom water did not correspond to higher rates of enzyme activity or heterotrophic bacterial productivity. Across sites, differences in hydrolysis rates and patterns were not due to temperature differences for either polysaccharide substrates ( $R^2 = 0.21$ , P = 0.26) or for peptide and glucose substrates ( $R^2 = 0.05$ , P = 0.59). Due to limited incubator capacity aboard ship, surface waters at all four stations were incubated at identical temperatures, but demonstrated distinct differences in hydrolysis rates and capacities (Table 1 and Figure 1). The highest polysaccharide hydrolysis rates measured at the first timepoint were from Stn. 2 bottom waters, the coldest station, which was also incubated at the lowest temperature in our experiments (Figure 3 and Table 1). Moreover, hydrolysis rates of glucosidase and peptidase substrates in Stn. 4 ring water were lower than in surface waters of Stns. 3 and 4, despite the fact that Stn. 4 bottom water had higher in situ and incubation temperatures (Table 1 and Figures 1, 2). Comparing stations, our data show differences that are independent of temperature in the spectrum of substrates that are hydrolyzed and hydrolysis rates, and may be more closely related to differences in functional capacities of the nascent microbial community. This observation

suggests that biogeochemical models that rely on temperature as the primary factor driving biogeochemical carbon cycling (e.g., Schimel, 2001), which would predict higher overall activities and heterotrophic bacterial production with increased warm core ring intrusions on the continental slope and shelf, would incorrectly predict biological effects on carbon cycling rates.

A previous investigation of microbial activities in the MAB that sampled waters originating from a Gulf Stream warm core ring in close proximity to the continental shelf (Bullock et al., 2015) indicates that the hydrolytic and heterotrophic bacterial productivity patterns observed in this study are a consistent feature of Gulf Stream-derived rings and intrusions. Bullock et al. (2015) found that the same spectrum of polysaccharides - pullulan, laminarin, xylan, and fucoidan were hydrolyzed after 2 days of incubation as in the present study, and heterotrophic bacterial productivity was also notably low in waters derived from the warm core ring compared to the other water masses sampled (13.4 ng C  $L^{-1}$   $h^{-1}$ , 16-39 fold lower compared to the other stations sampled). Although not all of the peptidase substrates used in the current study were also measured in Bullock et al. (2015), activities of leucine aminopeptidase, α-glucosidase, and β-glucosidase showed similar patterns to Stn. 4 bottom water, with moderate leucine aminopeptidase rates (ca. 12 nmol L<sup>-1</sup> h<sup>-1</sup> compared to 21.7 nmol  $L^{-1}$  h<sup>-1</sup> in this study) and very low  $\alpha$ - and β-glucosidase rates. These similarities were apparent despite differing temperatures (26.4°C compared to 12.0°C in this study) and season of sampling (November vs. April) between these studies. The similarity of hydrolytic rates and spectra, as well as the characteristically low heterotrophic bacterial productivity, in warm core ring waters across the current study as well as Bullock et al. (2015) suggests that water derived from warm core rings has a consistent, distinct biogeochemical imprint on the continental shelf. Other studies comparing heterotrophic bacterial productivity in water from farther offshore or from warm core ring sampling sites to coastal or shallower water sites (Baltar et al., 2009; Alonso-Sáez et al., 2012) also found that heterotrophic bacterial productivity was lower in water originating from North Atlantic Central Water, consistent with both Bullock et al. (2015) and this study.

The warm core ring intrusion events on the MAB originate from the Gulf Stream water and North Atlantic Central Water of the Sargasso Sea. Eddies in the Sargasso Sea have strong effects on net community production, carbon export, and microbial community composition and biomass (Benitez-Nelson and McGillicuddy, 2008; Ewart et al., 2008; Mouriño-Carballido, 2009; Nelson et al., 2014) that mirror the patterns observed in the ring-driven intrusion event at our sampling sites. These prior studies demonstrate that distinct bacterial distributions, biomass, and bacterial productivity are characteristic of eddies relative to surrounding water (Ewart et al., 2008; Mouriño-Carballido, 2009). These eddies are also associated with distinct microbial communities, as well as heterotrophic bacterial productivity in the same range as that observed in the current study (Nelson et al., 2014). The distinct community dynamics associated with eddy influences in the Sargasso Sea provide further evidence of the importance of mesoscale physical processes for bacterial distributions and protein production.

Several possible mechanisms may account for the observed differences in functional capabilities across water masses. These differences may be partially driven by biogeographical differences in microbial communities, with eddy or ring intrusions onto the continental shelf bringing with them a distinct microbial community (Nelson et al., 2014) with distinct hydrolytic capacities. The differences in functional capacities observed across sites and water masses are in keeping with functional biogeographical patterns in substrate hydrolysis previously identified across latitude, station, and depth (Arnosti et al., 2011, 2012; Hoarfrost and Arnosti, 2017), and between onshore and off-shore sites in the North Atlantic along similar scales of distance (D'Ambrosio et al., 2014). Differential longterm responses of the microbial communities in Stn. 4 surface and bottom waters to amendment with HMW DOM (Balmonte et al., 2019) indicate that these distinct water masses also have distinct microbial community structure and function, with differing potential impacts on the carbon cycle. These patterns in functional biogeography mirror biogeographical patterns in microbial community composition (Fuhrman et al., 2008; Zinger et al., 2011; Ladau et al., 2013; Nelson et al., 2014). Genetic evidence in support of linkages between community composition and function includes an investigation from the East China Sea, where communities in different water masses from shallow and bottom water depths on the continental shelf exhibited differential abundances of genes involved in hydrolysis of starch and chitin-derived carbon sources (Wang et al., 2017). In addition, in another study in the North Atlantic, the diversity of genes from glycosyl hydrolase family 5, one of the largest families of glycosyl hydrolases, differed significantly between the MAB and open ocean sites (Elifantz et al., 2008).

Differences in patterns of enzyme activities across water masses may also be affected by differences in organic matter composition and/or primary producer communities. For example, the MAB shelf is typically dominated by diatoms and dinoflagellates (Falkowski et al., 1994), whereas the North Atlantic open ocean typically harbors a higher number of cyanobacteria than in coastal regions (Lomas and Bates, 2004). These different taxa differ in organic matter composition (Biersmith and Benner, 1998), and thus may result in distinct water mass organic matter compositions that could also influence the activities of the nascent heterotrophic communities. Amendment with marine HMW DOM is known to induce shifts in microbial community composition and expression of genes involved in carbon cycling (McCarren et al., 2010), while amendment with diatom- vs. cyanobacterial-derived dissolved organic matter (DOM) induces different microbial community responses in terms of diversity and richness (Landa et al., 2014).

The distinct hydrolytic patterns in waters corresponding to the Gulf Stream ring intrusion in Stn. 4 bottom water, as it contrasts with hydrolytic patterns in continental shelf and shelf break waters, highlights the potential biogeochemical

importance and consequences of Gulf Stream interactions with the continental shelf. The distinct hydrolytic activities and functional capacities, coupled with low heterotrophic bacterial productivity, characteristic of ring intrusions will likely alter the amount and quality of carbon cycling on the continental shelf, shifting the composition of organic matter remineralized and possibly resulting in lower overall rates of remineralization along the Mid-Atlantic Bight shelf break during ring intrusions. In the future, the frequency of ring intrusions is likely to increase, due to the recent destabilization of the Gulf Stream (Andres, 2016) and the increasing number of warm core rings formed by the Gulf Stream (Monim, 2017). The frequency of ring intrusions onto the continental shelf, the amount of time that such intrusions persist (e.g., Ullman et al., 2014; Zhang and Gawarkiewicz, 2015), and the likely changes in carbon and nutrient cycling accompanying shifts in Gulf Stream meander and ring dynamics will thus have important effects on biogeochemical cycling along the Mid-Atlantic Bight in the coming years.

## **DATA AVAILABILITY**

Raw data underlying hydrolysis rates, bacterial productivity, and CTD casts are hosted on the BCO-DMO repository under the project title "Latitudinal and depth-related contrasts in enzymatic capabilities of pelagic microbial communities: Predictable patterns in the ocean?": http://www.bco-dmo.org/project/712359.

## REFERENCES

- Alderkamp, A.-C., van Rijssel, M., and Bolhuis, H. (2007). Characterization of marine bacteria and the activity of their enzyme systems involved in degradation of the algal storage glucan laminarin. FEMS Microbiol. Ecol. 59, 108–117. doi: 10.1111/j.1574-6941.2006.00219.x
- Alonso-Sáez, L., Sánchez, O., and Gasol, J. M. (2012). Bacterial uptake of low molecular weight organics in the subtropical Atlantic: are major phylogenetic groups functionally different? *Limnol. Oceanogr.* 57, 798–808. doi: 10.4319/lo. 2012.57.3.0798
- Andres, M. (2016). On the recent destabilization of the gulf stream path downstream of cape hatteras. Geophys. Res. Lett. 43, 9836–9842. doi: 10.1002/ 2016GL069966.Received
- Arnosti, C. (1996). A new method for measuring polysaccharide hydrolysis rates in marine environments. Org. Geochem. 25, 105–115. doi: 10.1016/S0146-6380(96)00112-X
- Arnosti, C. (2003). Fluorescent derivatization of polysaccharides and carbohydrate-containing biopolymers for measurement of enzyme activities in complex media. J. Chromatogr. B. Analyt. Technol. Biomed. Life Sci. 793, 181–191. doi: 10.1016/s1570-0232(03)00375-1
- Arnosti, C. (2011). Microbial extracellular enzymes and the marine carbon cycle. Ann. Rev. Mar. Sci. 3, 401–425. doi: 10.1146/annurev-marine-120709-142731
- Arnosti, C., Fuchs, B. M., Amann, R., and Passow, U. (2012). Contrasting extracellular enzyme activities of particle-associated bacteria from distinct provinces of the North Atlantic Ocean. Front. Microbiol. 3:425. doi: 10.3389/ fmicb.2012.00425
- Arnosti, C., Steen, A. D., Ziervogel, K., Ghobrial, S., and Jeffrey, W. H. (2011). Latitudinal gradients in degradation of marine dissolved organic carbon. *PLoS One* 6:e28900. doi: 10.1371/journal.pone.0028900
- Aylward, F. O., Eppley, J. M., Smith, J. M., Chavez, F. P., Scholin, C. A., and DeLong, E. F. (2015). Microbial community transcriptional networks are

## **AUTHOR CONTRIBUTIONS**

AH, GG, and CA designed the study. AH, JPB, SG, KZ, and CA conducted the field work, sample collection, and processing. AH analyzed the biological data. JB and GG processed and analyzed the physical oceanographic data. AH, GG, JB, and CA wrote the manuscript with input from all of the co-authors.

#### **FUNDING**

This study was funded by the NSF (OCE-1332881 and OCE-1736772 to CA; OCE-1657853 to GG), with additional funding provided by the DOE (DE-SC0013887).

## **ACKNOWLEDGMENTS**

We thank the captain and crew of the R/V *Endeavor* for their able assistance at sea, and the members of the scientific party of EN556 for their help with the shipboard work. We also thank Sarah Brown for making the ODV plot.

#### SUPPLEMENTARY MATERIAL

The Supplementary Material for this article can be found online at: https://www.frontiersin.org/articles/10.3389/fmars. 2019.00394/full#supplementary-material

- conserved in three domains at ocean basin scales. *Proc. Natl. Acad. Sci. U.S.A.* 112, 5443–5448. doi: 10.1073/pnas.1502883112
- Azam, F., and Malfatti, F. (2007). Microbial structuring of marine ecosystems. *Nat. Rev. Microbiol.* 5, 782–791. doi: 10.1038/nrmicro1747
- Azam, F., and Simon, M. (1989). Protein content and protein synthesis rates of planktonic marine bacteria. Mar. Ecol. Prog. Ser. 51, 201–213. doi: 10.3354/ meps051201
- Balmonte, J. P., Buckley, A., Hoarfrost, A., Ghobrial, S., Ziervogel, K., Teske, A., et al. (2019). Community structural differences shape microbial responses to high molecular weight organic matter. *Environ. Microbiol.* 21, 557–571. doi: 10.1111/1462-2920.14485
- Balmonte, J. P., Teske, A., and Arnosti, C. (2018). Structure and function of high Arctic pelagic, particle-associated and benthic bacterial communities. *Environ. Microbiol.* 20, 2941–2954. doi: 10.1111/1462-2920.14304
- Baltar, F., and Arístegui, J. (2017). Fronts at the surface ocean can shape distinct regions of microbial activity and community assemblages down to the bathypelagic zone: the azores front as a case study. Front. Mar. Sci. 4:252. doi: 10.3389/fmars.2017.00252
- Baltar, F., Arístegui, J., Gasol, J. M., Lekunberri, I., and Herndl, G. J. (2010a). Mesoscale eddies: hotspots of prokaryotic activity and differential community structure in the ocean. *ISME J.* 4, 975–988. doi: 10.1038/ismej.2010.33
- Baltar, F., Arístegui, J., Gasol, J. M, Sintes, E., van Aken, H., and Herndl, G. (2010b).
  High dissolved extracellular enzymatic activity in the deep central Atlantic Ocean. Aquat. Microb. Ecol. 58, 287–302. doi: 10.3354/ame01377
- Baltar, F., Arístegui, J., Sintes, E., van Aken, H. M., Gasol, J. M., and Herndl, G. J. (2009). Prokaryotic extracellular enzymatic activity in relation to biomass production and respiration in the meso- and bathypelagic waters of the (sub)tropical Atlantic. *Environ. Microbiol.* 11, 1998–2014. doi: 10.1111/j.1462-2920.2009.01922.x
- Benitez-Nelson, C. R., and McGillicuddy, D. J. (2008). Mesoscale physical-biological-biogeochemical linkages in the open ocean: an introduction to the

- results of the E-Flux and EDDIES programs. Deep Res. Part II Top. Stud. Oceanogr. 55, 1133–1138. doi: 10.1016/j.dsr2.2008.03.001
- Biersmith, A., and Benner, R. (1998). Carbohydrates in phytoplankton and freshly produced dissolved organic matter. Mar. Chem. 63, 131–144. doi: 10.1016/ S0304-4203(98)000577
- Bullock, A., Ziervogel, K., Ghobrial, S., Jalowska, A., and Arnosti, C. (2015). Microbial activities and organic matter degradation at three sites in the coastal North Atlantic: variations in DOC turnover times and potential for export off the shelf. Mar. Chem. 177, 388–397. doi: 10.1016/j.marchem.2015.06.023
- Chen, K., and He, R. (2010). Numerical investigation of the Middle Atlantic Bight shelfbreak frontal circulation using a high-resolution ocean hindcast model. *J. Phys. Oceanogr.* 40, 949–964. doi: 10.1175/2009jpo4262.1
- Chen, K., He, R., Powell, B. S., Gawarkiewicz, G. G., Moore, A. M., and Arango, H. G. (2014). Data assimilative modeling investigation of Gulf Stream Warm Core Ring interaction with continental shelf and slope circulation. *J. Geophys. Res. Oceans* 119, 5968–5991. doi: 10.1002/2014JC009898
- D'Ambrosio, L., Ziervogel, K., Macgregor, B., Teske, A., and Arnosti, C. (2014). Composition and enzymatic function of particle-associated and free-living bacteria: a coastal/offshore comparison. ISME J. 8, 2167–2179. doi: 10.1038/ ismei.2014.67
- Elifantz, H., Waidner, L. A., Michelou, V. K., Cottrell, M. T., and Kirchman, D. L. (2008). Diversity and abundance of glycosyl hydrolase family 5 in the North Atlantic Ocean. FEMS Microbiol. Ecol. 63, 316–327. doi: 10.1111/j.1574-6941. 2007.00429.x
- Etige, N. (2019). Understanding 38 years of Gulf Stream Warm Core Rings: Variability, Regimes, and Survival. M.S. Thesis, University of Massachusetts-Dartmouth: Dartmouth, MA, 76
- Ewart, C. S., Meyers, M. K., Wallner, E. R., McGillicuddy, D. J., and Carlson, C. A. (2008). Microbial dynamics in cyclonic and anticyclonic mode-water eddies in the northwestern Sargasso Sea. *Deep Res. Part II Top. Stud. Oceanogr.* 55, 1334–1347. doi: 10.1016/j.dsr2.2008.02.013
- Ezer, T., Atkinson, L. P., Corlett, W. B., and Blanco, J. L. (2013). Gulf Stream's induced sea level rise and variability along the U.S. mid-Atlantic coast. J. Geophys. Res. Oceans 118, 685–697. doi: 10.1002/jgrc.20091
- Falkowski, P. G., Biscaye, P. E., and Sancetta, C. (1994). The lateral flux of biogenic particles from the eastern North American continental margin to the North Atlantic Ocean. *Deep Sea Res. Part II Top. Stud. Oceanogr.* 41, 583–601. doi: 10.1016/0967-0645(94)900361
- Falkowski, P. G., Fenchel, T., and Delong, E. F. (2008). The microbial engines that drive Earth's biogeochemical cycles. *Science* 320, 1034–1039. doi: 10.1126/ science.1153213
- Fuhrman, J. A., Steele, J. A., Hewson, I., Schwalbach, M. S., Brown, M. V., Green, J. L., et al. (2008). A latitudinal diversity gradient in planktonic marine bacteria. *Proc. Natl. Acad. Sci. U.S.A.* 105, 7774–7778. doi: 10.1073/pnas.080307 0105
- Gawarkiewicz, G., Bahr, F., Beardsley, R. C., and Brink, K. H. (2001). Interaction of a slope eddy with the shelfbreak front in the Middle Atlantic Bight. *J. Phys. Oceanogr.* 31, 2783–2796. doi: 10.1175/1520-0485(2001)031<2783:IOASEW> 2.0.CO;2
- Gawarkiewicz, G., Todd, R. E., Zhang, W., Partida, J., Gangopadhyay, A., Monim, M.-U.-H., et al. (2018). The changing nature of shelfbreak exchange revealed by the OOI pioneer array. *Oceanography* 31, 60–70. doi: 10.5670/oceanog.2018.110
- Gawarkiewicz, G. G., Todd, R. E., Plueddemann, A. J., Andres, M., and Manning, J. P. (2012). Direct interaction between the Gulf Stream and the shelfbreak south of New England. Sci. Rep. 2:553. doi: 10.1038/srep00553
- Hoarfrost, A. (2017). Ahoarfrost/shelf1234: Shelf1234 Initial Release (Version v1.0.0). Zenodo. Available at: https://zenodo.org/record/580059# .XRN1DuszbIU (accessed May 15, 2017).
- Hoarfrost, A., and Arnosti, C. (2017). Heterotrophic extracellular enzymatic activities in the atlantic ocean follow patterns across spatial and depth regimes. Front. Mar. Sci. 4:200. doi: 10.3389/fmars.2017.00200
- Hoppe, H. (1983). Significance of exoenzymatic activities in the ecology of brackish water: measurements by means of methylumbelliferyl-substrates. *Mar. Ecol. Prog. Ser.* 11, 299–308. doi: 10.3354/meps011299
- Joyce, T. M., Bishop, J. K. B., and Brown, O. B. (1992). Observations of offshore shelf-water transport induced by a warm-core ring. *Deep Sea Res. Part A Oceanogr. Res. Pap.* 39, S97–S113. doi: 10.1016/S0198-0149(11)80007-5

- Kirchman, D. L. (2001). Measuring bacterial biomass production and growth rates from leucine incorporation in natural aquatic environments. *Methods Microbiol.* 30, 227–237. doi: 10.1016/s0580-9517(01)30047-8
- Ladau, J., Sharpton, T. J., Finucane, M. M., Jospin, G., Kembel, S. W., O'Dwyer, J., et al. (2013). Global marine bacterial diversity peaks at high latitudes in winter. *ISME J.* 7, 1669–1677. doi: 10.1038/ismej. 2013.37
- Landa, M., Cottrell, M. T., Kirchman, D. L., Kaiser, K., Medeiros, P. M., Tremblay, L., et al. (2014). Phylogenetic and structural response of heterotrophic bacteria to dissolved organic matter of different chemical composition in a continuous culture study. *Environ. Microbiol.* 16, 1668–1681. doi: 10.1111/1462-2920. 12242
- Lentz, S. J. (2003). A climatology of salty intrusions over the continental shelf from Georges Bank to cape hatteras. J. Geophys. Res. 108, 1–12. doi: 10.1029/ 2003jc001859
- Linder, C. A., and Gawarkiewicz, G. (1998). A climatology of the shelfbreak front in the Middle Atlantic Bight. J. Geophys. Res. 103, 18405–18423. doi: 10.1029/98jc 01438
- Lomas, M. W., and Bates, N. R. (2004). Potential controls on interannual partitioning of organic carbon during the winter/spring phytoplankton bloom at the bermuda atlantic time-series study (BATS) site. Deep Sea Res. Part I Oceanogr. Res. Pap. 51, 1619–1636. doi: 10.1016/j.dsr.2004.06.007
- Martinez-Garcia, M., Brazel, D. M., Swan, B. K., Arnosti, C., Chain, P. S. G., Reitenga, K. G., et al. (2012). Capturing single cell genomes of active polysaccharide degraders: an unexpected contribution of Verrucomicrobia. *PLoS One* 7:e35314. doi: 10.1371/journal.pone.0035314
- McCarren, J., Becker, J. W., Repeta, D. J., Shi, Y., Young, C. R., Malmstrom, R. R., et al. (2010). Microbial community transcriptomes reveal microbes and metabolic pathways associated with dissolved organic matter turnover in the sea. *Proc. Natl. Acad. Sci. U.S.A.* 107, 16420–16427. doi: 10.1073/pnas. 1010732107
- McGillicuddy, D. J. (2015). Mechanisms of physical-biological-biogeochemical interaction at the oceanic mesoscale. Ann. Rev. Mar. Sci. 8, 125–159. doi: 10. 1146/annurev-marine-010814-015606
- Monim, M. (2017). Seasonal and Inter-Annual Variability of Gulf Stream Warm Core Rings from 2000 to 2016. Ph.D. thesis, University of Massachusetts, Dartmouth.
- Mouriño-Carballido, B. (2009). Eddy-driven pulses of respiration in the Sargasso Sea. *Deep Res. Part I Oceanogr. Res. Pap.* 56, 1242–1250. doi: 10.1016/j.dsr.2009. 03.001
- Nelson, C. E., Carlson, C. A., Ewart, C. S., and Halewood, E. R. (2014). Community differentiation and population enrichment of Sargasso Sea bacterioplankton in the euphotic zone of a mesoscale mode-water eddy. *Environ. Microbiol.* 16, 871–887. doi: 10.1111/1462-2920.12241
- Obayashi, Y., and Suzuki, S. (2005). Proteolytic enzymes in coastal surface seawater: significant activity of endopeptidases and exopeptidases. *Limnol. Oceanogr.* 50, 722–726. doi: 10.4319/lo.2005.50.2.0722
- Ottesen, E. A., Young, C. R., Gifford, S. M., Eppley, J. M., Marin, R., Schuster, S. C., et al. (2014). Multispecies diel transcriptional oscillations in open ocean heterotrophic bacterial assemblages. *Science* 345, 207–212. doi: 10.1126/science. 1252476
- Redfield, A. C. (1958). The biological control of chemical factors in the environment. Sci. Prog. 11, 150–170.
- Schimel, J. P. (2001). "Biogeochemical models: implicit vs. explicit microbiology," in *Global Biogeochemical Cycles in the Climate System*, eds E. D. Schulze, S. P. Harrison, M. Heimann, E. A. Holland, J. J. LLoyd, I. C. Prentice, et al. (San Diego, CA: Academic Press), 177–183.
- Schlitzer, R. (2016). Ocean Data View. Available at: http://odv.awi.de
- Steen, A. D., Ziervogel, K., Ghobrial, S., and Arnosti, C. (2012). Functional variation among polysaccharide-hydrolyzing microbial communities in the Gulf of Mexico. *Mar. Chem.* 13, 13–20. doi: 10.1016/j.marchem.2012. 06.001
- Ullman, D. S., Codiga, D. L., Pfeiffer-Herbert, A., and Kincaid, C. R. (2014). An anomalous near-bottom cross-shelf intrusion of slope water on the southern New England continental shelf. J. Geophys. Res. Ocean 119, 1739–1753. doi: 10.1002/2013JC009259
- Wang, Y., Zhang, R., He, Z., Van Nostrand, J. D., Zheng, Q., Zhou, J., et al. (2017).Functional gene diversity and metabolic potential of the microbial community

- in an estuary-shelf environment. *Front. Microbiol.* 8:1153. doi: 10.3389/fmicb. 2017.01153
- Wegner, C.-E., Richter-Heitmann, T., Klindworth, A., Klockow, C., Richter, M., Achstetter, T., et al. (2013). Expression of sulfatases in *Rhodopirellula baltica* and the diversity of sulfatases in the genus *Rhodopirellula*. *Mar. Genomics* 9, 51–61. doi: 10.1016/j.margen.2012.12.001
- Wright, W. R., and Parker, C. E. (1976). A volumetric temperature/salinity census for the middle Atlantic Bight. *Limnol. Oceanogr.* 21, 563–571. doi: 10.4319/lo. 1976.21.4.0563
- Zhang, W. G., and Gawarkiewicz, G. (2015). Dynamics of the direct intrusion of gulf stream ring water onto the mid-atlantic bight shelf. Geophys. Res. Lett. 42, 7687–7695. doi: 10.1002/2015GL06 5530
- Zhang, W. G., McGillicuddy, D. J., and Gawarkiewicz, G. G. (2013). Is biological productivity enhanced at the New England shelfbreak front? *J. Geophys. Res. Oceans* 118, 517–535. doi: 10.1002/jgrc.20068

- Zinger, L., Amaral-Zettler, L. A., Fuhrman, J. A., Horner-Devine, M. C., Huse, S., Welch, D. B. M., et al. (2011). Global patterns of bacterial beta-diversity in seafloor and seawater ecosystems. *PLoS One* 6:e24570. doi: 10.1371/journal. pone.0024570
- **Conflict of Interest Statement:** The authors declare that the research was conducted in the absence of any commercial or financial relationships that could be construed as a potential conflict of interest.

Copyright © 2019 Hoarfrost, Balmonte, Ghobrial, Ziervogel, Bane, Gawarkiewicz and Arnosti. This is an open-access article distributed under the terms of the Creative Commons Attribution License (CC BY). The use, distribution or reproduction in other forums is permitted, provided the original author(s) and the copyright owner(s) are credited and that the original publication in this journal is cited, in accordance with accepted academic practice. No use, distribution or reproduction is permitted which does not comply with these terms.